JOURNAL OF SOLID STATE CHEMISTRY 100, 371–378 (1992)

Lithium Insertion into $YBa_2Cu_3O_7$

M. S. ISLAM[1] AND C. ANANTHAMOHAN

Department of Chemistry, University of Surrey, Guildford, GU2 5XH, United Kingdom

Received October 16, 1991; in revised form June 8, 1992; accepted June 24, 1992

Atomistic computer simulation techniques are used to investigate the effects of lithium insertion into $YBa_2Cu_3O_7$. Attention is focused on various possible lattice sites occupied by the inserted lithium ions and pathways for their migration. The square-planar position in the Cu(2) layer is calculated to be the most energetically favorable. This is supported by the structural modeling of the ordered lithiated phase $Li_{0.33}YBa_2Cu_3O_7$. The calculated activation energies derived from migration profiles are in accord with experimental values and suggest fairly mobile lithium ions. © 1992 Academic Press, Inc.

Introduction

Lithium insertion into host compounds has received much attention for a number of years, in part due to their potential applications as solid electrolytes in secondary batteries. Such insertion reactions allow the low-temperature synthesis of novel materials that may not be possible by any high-temperature method, as well as providing a unique approach to changing the properties of host compounds with minimal structural rearrangement. The most widely studied intercalation compounds have been the transition metal dichalcogenides (*1–3*) and spinel oxides (*4–6*). It is now well established that for insertion reactions to occur the host structure requires three main characteristics: suitable lattice sites for the guest ion to occupy, adequate ion diffusion paths, and cations that can be easily reduced.

The possibility of developing new high-T_c materials or improving the superconducting properties of the $YBa_2Cu_3O_7$ host has resulted in some recent studies of lithium insertion into this system. The structure of $YBa_2Cu_3O_7$ shows features that are well suited to insertion chemistry: a layered perovskite-like lattice containing interstitial sites and diffusion paths, and mixed oxidation states for copper. It is worthwhile noting that lithium insertion into $YBa_2Cu_3O_7$ is not surprising in view of the similarity between the superconducting oxides and conventional ceramic oxides in a wide range of defect phenomena, as discussed by Stoneham and Smith (*7*).

Early lithium insertion studies by Eichenbusch *et al.* (*8*) using electrochemical techniques found the reaction proceeding topotactically to a composition of $Li_{0.33}YBa_2Cu_3O_7$. Vondrak *et al.* (*9*) have also reported electrochemical measurements and obtained a lithiated product of $Li_{0.45}YBa_2Cu_3O_7$, with a diffusion coefficient, $D_{Li} \sim$

[1] To whom correspondence should be addressed.

0022-4596/92 $5.00

10^{-12} cm^2 sec^{-1}. By chemical insertion at room temperature Alario-Franco *et al.* (*10*) formed $Li_xYBa_2Cu_3O_7$ in which superconductivity and ionic conductivity coexist for low lithium concentrations ($x \leq 0.4$), but not within the same temperature range; the lithiated material is a superconductor at T ~ 90 K and a lithium ion conductor at $T > 400$ K. Powder X-ray diffraction and electron microscopy experiments on these samples showed that lithium insertion had little effect on the structure in the *ab*-plane with the *c*-axis increasing slightly. More recently, ionic conductivity measurements (*11*) using dielectric response techniques derived an activation energy of ~0.7 eV for lithium ion migration. Note that in addition to lithium insertion there have been some similar studies of hydrogen insertion into $YBa_2Cu_3O_7$ (*8, 12*) and iodine intercalation of $Bi_2Sr_2CaCu_2O_8$ (*13*).

In evaluating the influence of insertion processes on the structural and transport properties of the host material, it is important to know the precise location of the guest ion. However, X-ray diffraction experiments have difficulty extracting this information due to the low scattering power of X-rays by the light lithium ions. Similarly, the nature of the atomistic mechanism or migration path controlling lithium ion diffusion is still uncertain.

In an attempt to clarify these issues we report a computer simulation study of lithium insertion into $YBa_2Cu_3O_7$. These techniques are particularly suited to probing structures and migration mechanisms at the atomic level, and have been successfully applied to defect studies of a wide range of polar solids including La_2CuO_4 (*14, 15*), $Ba_{1-x}K_xBiO_3$ (*16*), and $Ca_{0.85}Sr_{0.15}CuO_2$ (*17*). The present study extends our previous modeling work on dopant substitution (*18, 19*) and oxygen transport (*20*) in $YBa_2Cu_3O_7$ by examining possible sites occupied by the intercalating lithium ions and various paths for their migration.

2. Theoretical Methods

The lattice simulations were performed using the widely used CASCADE code which employs the generalized Mott–Littleton methodology and is discussed in greater detail elsewhere (*21, 22*). In addition to a variety of defect studies, these techniques have been applied to analogous studies of alkali-metal insertion into Fe_3O_4 (*23*), WO_3 (*24*), and α-U_3O_8 (*25*).

The calculations are formulated within the framework of the Born model for the crystalline solid, and require specification of interatomic potentials representing the interaction between host lattice ions and between host and defect (guest) species. The effective potentials are generally represented by the following pair-wise function:

$$\phi_{ij} = \frac{Z_i Z_j e^2}{r_{ij}} + A_{ij}\exp(-r_{ij}/\rho_{ij}) - C_{ij}/r_{ij}^6. \quad (1)$$

The first term is the long-range Coulombic interaction which is summed by the Ewald method to improve convergence. The second term describes the short-range repulsive forces which arise from the overlap of electron clouds. The final term concerns the attractive van der Waals forces which, in practice, also incorporates small covalency effects. Ionic polarization is treated by the shell model (*26*) in which the ion is considered as a massless shell surrounding a massive core and are coupled to each other by means of a harmonic spring. Polarization of the ion then occurs through the displacement of the shell relative to the core.

An important feature of the insertion calculations is the treatment of lattice relaxation about the guest species. The Mott–Littleton approach (*21, 27*) is to divide the host lattice into two regions so that ion interactions in the central inner region (I) immediately around the defect are calculated explicitly, whereas the remainder of the crystal (region II), where the forces exerted

by the defect are weak, is treated as a dielectric continuum. In this study, region I contained 225 ions, which was found to be adequate for convergence of the computed energies.

The interatomic potentials and shell model parameters for $YBa_2Cu_3O_7$ are those used in our previous simulation studies (*18–20, 28*) which correctly reproduce the observed orthorhombic structure and predicted well the effects of dopant substitution. Most recently, these potentials have been used in a study of Fe^{3+} clustering in $YBa_2Cu_3O_7$ (*19*). The parameters representing the $Li^+ \ldots O^{2-}$ interaction were derived by empirical methods for the anti-fluorite structured Li_2O (*23*) and were successfully applied to a similar study of lithium insertion into Fe_3O_4 spinel.

Finally in this section, we note that calculations were carried out in parallel using an alternative Li–O potential from a study of $LiNbO_3$ (*29*), and a Li–Ba potential from electron-gas calculations, both of which, resulted in the same overall conclusions and, in most cases, good quantitative agreement (*30*).

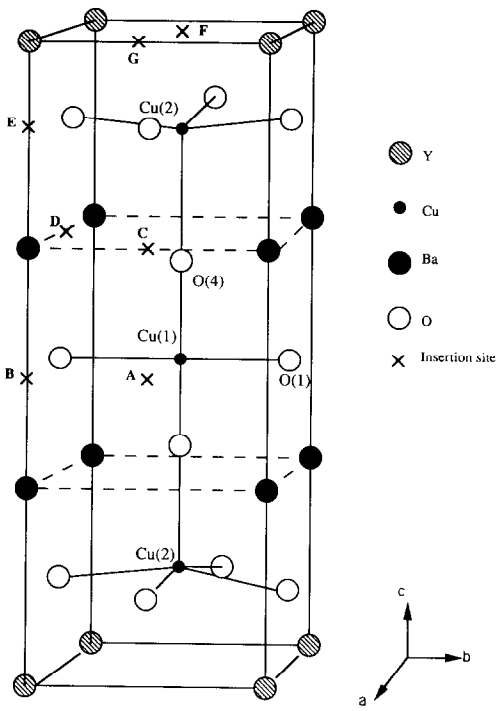

FIG. 1. Unit cell of $YBa_2Cu_3O_7$ indicating the lithium insertion sites considered.

3. Results and Discussion

3.1. Insertion Sites

Within the framework of the $YBa_2Cu_3O_7$ structure we have identified a number of possible sites that may be occupied by the inserted lithium ions. These are indicated in Fig. 1 with their coordinates listed in Table I. The type and number of nearest-neighbor oxygen ions, as well as the corresponding Li–O separations, are also included in Table I.

It can be seen that sites A and B are associated with the *b*-axis "tunnel" in the Cu(1) layer; C and D are in the Ba layer; site E is in the Cu(2) plane and has a square-planar coordination, whereas F and G are both in the oxygen-deficient Y layer. These seven sites show a variety of Li–O separations ranging from 1.4 to 2.7 Å. We note that Alario-Franco *et al.* (*10*) also identified possible positions which, in our notation, correspond to sites A, B, D, and E.

To determine preferred insertion positions an unambiguous interpretation of any structural data can be difficult. This problem can be investigated by theoretical methods since relative energetics of interstitial formation can be computed.

In Table II we present the results of calculated energies of isolated lithium ions at all the proposed insertion sites. The energies are associated with introducing a lithium ion to the lattice site from infinity, and include contributions from electrostatic and short-range terms, as well as the important effect of lattice relaxation around the guest species. Examination of their relative magnitude reveals that the most favourable posi-

TABLE I

POSSIBLE LITHIUM INSERTION SITES IN THE $YBa_2Cu_3O_7$ STRUCTURE

Insertion Site[a]	Neighboring oxygen ions	Li–O separation (Å)
A (0.5, 0, 0)	O(1) × 4	2.653
	O(4) × 4	2.722
B (0.5, 0.508252, 0)	O(1) × 2	1.909
C (0.5, 0, 0.565904)	O(2)	2.241
	O(4) × 2	1.935
D (0, 0.508252, 0.565904)	O(1)	2.160
	O(3)	2.242
	O(4) × 2	1.966
E (0.5, 0.508252, 1.046037)	O(2) × 2	1.983
	O(3) × 2	1.952
F (0, 0, 1.52617)	O(2) × 4	2.382
	O(3) × 4	2.407
G (0.5, 0, 1.52617)	O(2) × 2	1.425

[a] Atomic coordinates in lattice units (a_o).

tion is site E, which is lower in energy than site D by 0.2 eV. This result suggests that the square-planar position (E) would be preferentially occupied on lithiation, especially at higher temperatures where there are fewer kinetic constraints. Interestingly, this site has Li–O separations (~2 Å) that are slightly longer than the Li–O bond lengths (1.59 Å) in the Li_2O anti-fluorite structure in which lithium is also four-coordinate (*31*).

TABLE II

CALCULATED DEFECT ENERGY AND DISPLACEMENT OF ISOLATED LITHIUM IONS

Insertion site	Displacement (Å)[a]	E(eV)
A	0.25 (−z)	−0.30
B	0	−1.96
C	0.84 (+z)	−2.64
D	0.66 (+z)	−3.00
E	0	−3.20
F	0	−2.71
G	0	−2.30

[a] Displacement with respect to coordinates in Table I and the direction in parentheses.

It is important to note that the simulation of isolated lithium ions correspond to very low concentrations, the results of which may not be directly comparable with experimental studies on highly lithiated compounds. The effect of long-range ordering of lithium ions could result in a different site being preferentially occupied than that predicted above. We have, therefore, carried out perfect lattice simulations on ordered phases of $Li_{0.33}YBa_2Cu_3O_7$ for the individual insertion sites considered.

3.2. *Modeling of $Li_{0.33}YBa_2Cu_3O_7$*

The initial structure of the lithiated phase is constructed from the unperturbed $YBa_2Cu_3O_7$ structure with the Li ions occupying the appropriate lattice sites. Hence, the basis representing $Li_{0.33}YBa_2Cu_3O_7$ consists of 40 ions derived from tripling the normal $YBa_2Cu_3O_7$ unit cell in the a-direction with one of the copper ions in the chain treated as Cu^+. Note that the lithium is completely ionized with the donated electron localized on the copper chain site. Indeed, previous studies have shown that the presence of re-

TABLE III

CALCULATED LATTICE ENERGIES OF THE INSERTION COMPOUNDS $Li_{0.33}YBa_2Cu_3O_7$

Lithium site	U_L (eV)
A	NC[a]
B	−253.52
C	−254.03
D	−254.79
E	−255.17
F	−254.10
G	−254.20
$YBa_2Cu_3O_7$	−259.86

[a] Non-convergence of simulation.

ducible cations facilitates the uptake of lithium (*1–3*).

The lattice simulation then involves relaxing the structure to a minimum energy configuration under constant pressure conditions, i.e., allowing the lattice vectors and atomic coordinates to vary during the energy minimization procedure. The resulting lattice energies of $Li_{0.33}YBa_2Cu_3O_7$ for each of the seven insertion sites are reported in Table III. This shows that the structure in which the lithium ions occupy site E emerges as the most stable structure, in accord with the results for the isolated intercalate. Furthermore, the difference in lattice energies (ΔU_L) between this phase and $YBa_2Cu_3O_7$ is found to be 4.76 eV. For comparison the energetics for the formation of an isolated pair of Li^+ and Cu^+ ions can also be derived and found to be 5.04 eV. Therefore, ΔU_L is ~0.3 eV lower in energy and confirms the energetic preference for the long-range ordering of lithium ions.

In Table IV the calculated cell parameters for $Li_{0.33}YBa_2Cu_3O_7$ are compared with values for $YBa_2Cu_3O_7$. This shows a significant increase in the *c*-axis with a corresponding volume expansion of ~4%. The orthorhombic structure is only slightly modified with a *b*/*a* ratio of 1.03. These results are consistent with diffraction and electron microscopy studies (*10*) which find that on lithiation the major increase (or disorder) occurs along the *c*-axis.

TABLE IV

CALCULATED UNIT CELL DIMENSIONS

Compound	*a* (Å)	*b* (Å)	*c* (Å)	*V* (Å^3)
$YBa_2Cu_3O_7$	3.8235	3.8524	11.7304	172.78
$Li_{0.33}YBa_2Cu_3O_7$ (site E)	3.7578	3.8538	12.4375	180.12

3.3. Lithium Ion Migration

Insertion processes are also dependent upon the mobility of the intercalate through the host lattice. Fast diffusion of the guest ions depends on the availability of favourable migration pathways. We have, therefore, identified various possible pathways for lithium diffusion in the $YBa_2Cu_3O_7$ lattice. The five mechanisms considered are essentially direct jumps between neighbouring interstitial sites: mechanism I involves migration along the *b*-axis in the Cu(1) layer (Fig. 2); mechanisms II and III are associated with jumps in the Ba and Y layers,

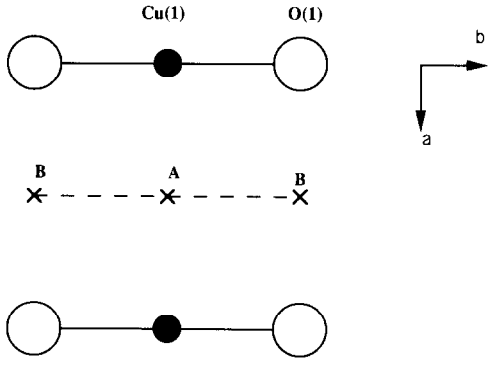

FIG. 2. Migration pathway in the Cu(1) layer (Mechanism I).

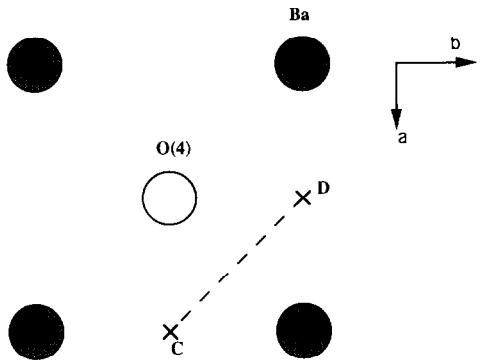

FIG. 3. Migration pathway in the Ba layer (Mechanism II).

TABLE V

CALCULATED ACTIVATION ENERGIES FOR LITHIUM ION MIGRATION

Mechanism	Layer	E_a (eV)
I (A–B)	Cu(1)	1.66
II (C–D)	Ba	0.78
III (F–G)	Y	0.59
IV (E–F)	Interlayer	1.45
V (A–C)	*c*-Axis	2.34

respectively (Figs. 3 and 4); mechanism IV involves an interlayer jump between sites E and F, since intralayer migration between the E sites is highly restricted; finally, mechanism V concerns migration along the *c*-axis between sites A and C.

The energy barriers to migration are evaluated by calculating the defect energy of the lithium ion at positions along the migration path. In this way potential energy profiles can be mapped out for each of the mechanisms considered. Migration activation energies were then derived from the "saddle-point" in such profiles and are reported in Table V.

Examination of the results shows that mechanism III in the Y layer emerges as the lowest energy path with a mean migration energy of 0.59 eV; the *a*- and *b*-axis components of this value are 0.64 and 0.55 eV, respectively. Lithium ion migration in the Ba layer involving the insertion sites C and D is also found to have a favorable energy barrier of 0.78 eV. These values suggest relatively high mobility of lithium ions in the $YBa_2Cu_3O_7$ lattice. Moreover, the calculated energies are in line with observed activation energies of 0.5 and 0.7 eV from dc conductivity and complex impedance measurements respectively (*10, 11*), which the authors associate with lithium ion motion. However, we are aware that the occupancy of site F at equilibrium would involve some energy term for transfer from the preferred site and would be included in experimental conductivity terms. This may lead to a greater difference between our calculated migration energy and experimental values.

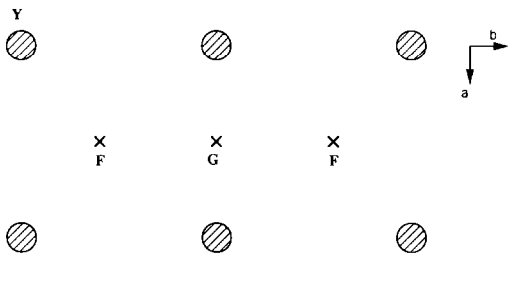

FIG. 4. Migration pathway in the Y layer (Mechanism III).

We note that the diffusion rate is likely to be slower than that found in more pronounced layered structures such as TiS_2 (*1*), which have greater flexibility in the *c*-direction. Indeed, Vondrak *et al.* (*9*) estimated a value of the diffusion coefficient, $D_{Li} \sim 10^{-12}$ $cm^2\ s^{-1}$, for $Li_{0.45}YBa_2Cu_3O_7$ which they suggest is more commonly found in tunnel or framework structures rather than layered materials. In any event, long-range lithium diffusion is predicted to be dominated by transport in the *ab*-plane with high energy barriers to *c*-axis migration. In view of this type of motion anisotropic diffusion is ex-

pected, but not surprising, in single crystalline $Li_xYBa_2Cu_3O_7$.

4. Conclusions

The present study demonstrates how atomistic simulation techniques can be used to examine lithiation of $YBa_2Cu_3O_7$ and thus provide information on various insertion and diffusion processes.

Three principal conclusions emerge from our discussion. First, the energetics of isolated lithium ions suggest that the intercalate will preferentially occupy the square-planar position in the Cu(2) plane, being slightly more favorable than the four-coordinate site in the Ba layer. This prediction is supported by the perfect lattice modelling of the ordered phase $Li_{0.33}YBa_2Cu_3O_7$.

Second, the structural modeling of the lithiated phase confirms the long-range ordering of lithium ions. The basic structure of $YBa_2Cu_3O_7$ remains intact with a slight increase of the c-parameter which is consistent with results of diffraction studies.

Finally, the calculations find lithium ion migration in the Y layer energetically favourable with an activation energy of 0.6 eV, which is in line with experimental values. These results suggest fairly fast and anisotropic lithium ion diffusion, although slower than those exhibited in more pronounced layered materials.

Acknowledgments

The calculations were performed on the Cray-XMP supercomputer at the University of London Computer Centre. One of us (CA) is supported by a University of Surrey Major Award.

We are grateful to Cathy Bintz for assistance in the final stages of this work.

References

1. F. Levy (Ed.), "Intercalated Layered Compounds, Reidel, Dordrecht (1979).
2. M. S. Whittingham, *Science* **192,** 1126 (1976).
3. M. S. Whittingham, *Prog. Solid State Chem.* **12,** 91 (1978).
4. R. J. Cava, D. W. Murphy, S. Zahurak, A. Santoro, and R. S. Roth, *J. Solid State Chem.* **53,** 64 (1984).
5. C. J. Chen, M. Greenblatt, and J. V. Waszczak, *Mater. Res. Bull.* **21,** 609 (1986).
6. W. I. F. David, M. M. Thackeray, L. A. De Picciotto, and J. B. Goodenough, *J. Solid State Chem.* **67,** 316 (1987).
7. A. M. Stoneham and L. W. Smith, *J. Phys. Condens. Mater.* **3,** 225 (1991).
8. H. Eichenbusch, W. Paulus, E. Gocke, J. F. March, H. Koch, and R. Schoellhorn, *Angew. Chem. Int. Ed. Engl.* **26,** 1188 (1987).
9. J. Vondrak, I. Jakubec, J. Bludska, and V. Skacel, *Electrochim. Acta* **35,** 995 (1990).
10. M. A. Alario-Franco, E. Moran, A. Varez, J. Santamaria, and F. Sanchez-Quesada, *Solid State Ionics* **44,** 73 (1990).
11. A. Varez, E. Moran, M. A. Alario-Franco, J. Santamaria, G. Gonzalez-Diaz, and F. Sanchez-Quesada, *Solid State Commun.* **76,** 917 (1990).
12. M. Nicolas, J. N. Daou, I. Vedel, P. Vajda, J. P. Burger, J. Lesueur, and L. Dumoulin, *Solid State Commun.* **66,** 1157 (1988).
13. X. D. Xiang, S. McKernan, W. A. Vareka, A. Zettl, J. L. Corkill, T. W. Barbee, and M. L. Cohen, *Nature* **348,** 145 (1990).
14. M. S. Islam, M. Leslie, S. M. Tomlinson, and C. R. A. Catlow, *J. Phys. C* **21,** L109 (1988).
15. N. L. Allan and W. C. Mackrodt, *Philos. Mag A* **58,** 555 (1988).
16. X. Zhang and C. R. A. Catlow, *Physica C* **173,** 25 (1991).
17. S. J. L. Billinge, P. K. Davies, T. Egami, and C. R. A. Catlow, *Phys. Rev. B* **43,** 10340 (1991).
18. M. S. Islam and R. C. Baetzold, *Phys. Rev. B* **40,** 10926 (1989).
19. M. S. Islam and C. Ananthamohan, *Phys. Rev. B* **44,** 9492 (1991).
20. M. S. Islam, *Supercond. Sci. Technol.* **3,** 531 (1990).
21. C. R. A. Catlow, *in* "Solid-State Chemistry: Techniques" (A. K. Cheetham and P. Day, Eds.), Chap. 7, Oxford Univ. Press (Clarendon), London/New York (1987).
22. C. R. A. Catlow, *Annu. Rev. Mater. Sci.* **16,** 517 (1986).
23. M. S. Islam and C. R. A. Catlow, *J. Solid State Chem.* **77,** 180 (1988).
24. J. C. Newton-Howes and A. N. Cormack, *J. Solid State Chem.* **79,** 12 (1989).
25. R. G. J. Ball and P. G. Dickens, *J. Mater. Chem.* **1,** 415 (1991).

26. B. G. DICK AND A. W. OVERHAUSER, *Phys. Rev.* **112,** 90 (1958).
27. A. B. LIDIARD, *J. Chem. Soc., Faraday Trans. 2* **85,** 341 (1989).
28. R. C. BAETZOLD, *Phys. Rev B* **38,** 11304 (1988); **42,** 56 (1990).
29. H. DONNERBERG, S. M. TOMLINSON, C. R. A. CATLOW, AND O. F. SCHIRMER, *Phys. Rev. B* **40,** 11909 (1989).
30. C. BINTZ AND M. S. ISLAM, unpublished results.
31. A. F. WELLS, "Structural Inorganic Chemistry," Clarendon Press, Oxford (1984).